WARWICK
THE UNIVERSITY OF WARWICK

Original citation:
Kellner, Quirin, Worwood , D, Widanage, D. W. and Marco, James (2017) Electrical and thermal behaviour of pouch-format lithium ion battery cells under high-performance and standard automotive duty-cycles. In: IEEE Vehicle Power and Propulsion Conference, Belfort, France, 11-14 Dec 2017. Published in: IEEE Vehicle Power and Propulsion Conference (In Press)
Permanent WRAP URL:
http://wrap.warwick.ac.uk/95971

Copyright and reuse:
The Warwick Research Archive Portal (WRAP) makes this work by researchers of the University of Warwick available open access under the following conditions. Copyright © and all moral rights to the version of the paper presented here belong to the individual author(s) and/or other copyright owners. To the extent reasonable and practicable the material made available in WRAP has been checked for eligibility before being made available.

Copies of full items can be used for personal research or study, educational, or not-for profit purposes without prior permission or charge. Provided that the authors, title and full bibliographic details are credited, a hyperlink and/or URL is given for the original metadata page and the content is not changed in any way.

Publisher's statement:
"© 2017 IEEE. Personal use of this material is permitted. Permission from IEEE must be obtained for all other uses, in any current or future media, including reprinting /republishing this material for advertising or promotional purposes, creating new collective works, for resale or redistribution to servers or lists, or reuse of any copyrighted component of this work in other works."

A note on versions:
The version presented here may differ from the published version or, version of record, if you wish to cite this item you are advised to consult the publisher's version. Please see the 'permanent WRAP URL' above for details on accessing the published version and note that access may require a subscription.

For more information, please contact the WRAP Team at: wrap@warwick.ac.uk

warwick.ac.uk/lib-publications

Electrical and thermal behavior of pouch-format lithium ion battery cells under high-performance and standard automotive duty-cycles

Quirin Kellner, Daniel Worwood, W. Dhammika Widanage, James Marco

WMG

Warwick University

Coventry, United Kingdom

E-Mail: Q.kellner@warwick.ac.uk

***Abstract*—Six pouch-format cells comprising a carbon anode and nickel-cobalt-manganese (NCM) cathode are characterized. Their 1C discharge capacity and open circuit voltage are determined. Internal Resistance is investigated via Hybrid Pulse Power Characterization tests and Electrochemical Impedance Spectroscopy. They are subsequently subject to two different electrical loading profiles, one representing high-performance (HP) driving applications, the other representing urban and extra-urban driving scenarios. The cells are instrumented with thermocouples to determine their surface temperature during cycling. The experimental results show that HP scenarios result in higher temperatures and temperature gradients, requiring bespoke thermal management strategies and suggesting increased degradation over prolonged use.**

Keywords—lithium ion battery; NCM; characterisation; thermal; high-performance

I. INTRODUCTION

Recent developments in lithium-ion battery (LIB) technology have opened up the high performance (HP) vehicle market to battery electric vehicles (BEVs) [1]. Use cases within the HP vehicle environment such as racing applications are fundamentally different to normal driving. For these scenarios, existing testing procedures are not sufficient to gather reliable data regarding thermal and electrical behavior. As a result it is necessary to use tailored testing profiles to evaluate batteries for the HP segment [2].

The majority of research regarding the electrical and thermal behavior of LIBs for EVs as presented within [3]–[5] focusses on the behavior of cells under steady state conditions, e.g. "normal driving" conditions and urban scenarios. As such, the electrical and thermal behavior of batteries under realistic HP duty cycles is not well understood. Recent publications by Worwood et al. [6], [7] have considered the track driving use case within simulation studies targeting thermal management and have identified the need for active thermal management during these cases. However, there is no published experimental data of batteries in track driving applications available. This research targets this knowledge gap by investigating large pouch format NCM cells undergoing a HP duty profile representing racing applications and the IEC 62660 cycle life profile A [8].

This paper is structured as follows: Section II presents the experimental set-up testing procedures for characterization and performance tests. The test results are presented and discussed within section III, and the conclusions and further work recommendations comprise section IV.

II. METHODOLOGY

Six pouch-format LIB cells comprising a graphite anode and a lithium-nickel-manganese-cobalt-oxide (NCM) cathode are tested to determine their thermal and electrical performance when they are subjected to a duty cycle representing "HP driving" applications and a duty cycle representing "normal driving" applications.

A. Duty Cycle Description

The duty cycle representing HP applications is shown in Fig. 1a. It is derived from a database of battery duty cycles using a frequency-time swapping algorithm presented within [9]. The database itself consists of battery profile simulations of a high-performance BEV driving on 12 different racing circuits, generated using the commercially available software IPG CarMaker as outlined in [2]. The duty cycle representing normal driving is the *"Cycle-life testing profile A"* as described within [8] and is shown in Fig. 1b. The values on the vertical axis for both cycles represent normalized power demand as drawn from the battery with negative values indicating discharging and positive values representing charging. A value of -1 represents a discharging demand of -100% of the battery test power as defined in the IEC 62660 standard [8].

The HP cycle reaches peak power demand for charging and discharging more frequently compared to the IEC profile. This corresponds well with the expected behavior of driving on a track. Charging and discharging pulses are in quick succession with only a few seconds in between peak power demand and little to no cell relaxation periods exist for the duration of driving. In contrast, discharging and charging pulses within the

IEC profile are encompassed by resting periods allowing cell relaxation.

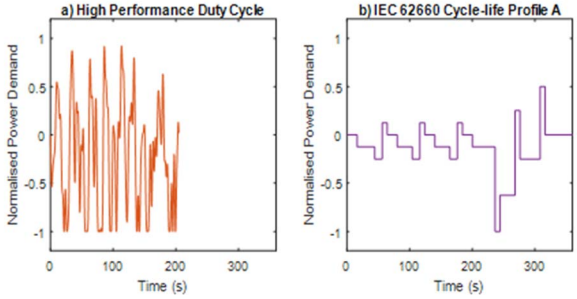

Fig. 1 a) A HP duty cycle representing typical track-driving application; b) IEC 62660 cycle life profile representing typical normal driving scenario

B. *Thermal considerations*

The high currents during charging and discharging result in cell self-heating (Q_h) due to irreversible heat generation [6] as given in (1).

$$Q_h = I^2.R \tag{1}$$

I is the cell current in Ampere, and R the internal resistance of the cell in Ohm. The temperature (T) of the battery can be calculated as a function of time as given in

$$MC_p^m \frac{dT}{dt} = Q_h - hA(T - T_\infty) \tag{2}$$

M is the mass of the cell in kg, h is the heat transfer battery coefficient between the batter and its surroundings in W.m^{-2}.K^{-1}, A is the surface are of the cell affected by heat transfer, C_p^m is the mean heat capacity of the battery in J.K^{-1}.kg^{-1}, and T_∞ is the temperature of the surroundings in K.

The increased intensity of the HP duty cycle profile is expected to manifest itself in the cell temperature. High temperatures are a primary reason for battery degradation [10] and understanding the extent to which cell self-heating occurs is an important factor for thermal management and battery pack considerations.

It is also well known that cells cycled under dynamic electrical loading profiles do not experience uniform heat generation and temperature development throughout the cell [11]. Areas of the cell which are at elevated temperatures display lower internal resistances originating from mass transport effects within the cell. Subsequently those areas are subject to larger current densities than their surroundings, and over time display higher rates of degradation [12].

C. *Experimental Set-Up*

A CAD drawing of the test rig, cooling fins and cooling plate, as well as a photo of the assembled test rig is shown in Fig. 2.

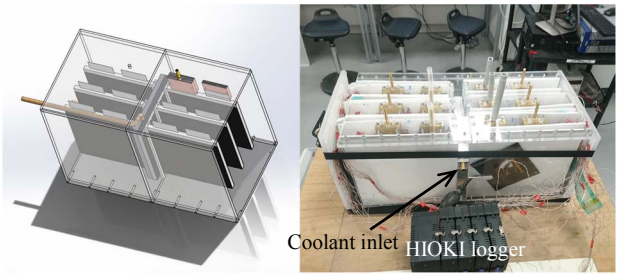

Fig. 2 a: CAD drawing of test rig design with cells. b: photo of assembled test rig with HIOKI temperature logger

Cells are suspended from the rig ceiling, fixed by their tabs. The cells are thermally isolated from each other using Styrofoam and a thermally insulating material (foam-glass). All tests are conducted in a thermal chamber at 20°C.

Due to the intensity of the HP cycling profiles a cooling system is employed during testing as a safety mechanism. Cooling of the cells is achieved via indirect fin cooling. The front and back faces of each pouch cell is in contact with a

TABLE I
CHARACTERIZATION AND PERFORMANCE TESTS FOR BATTERIES UNDERGOING HP DUTY CYCLING AND IEC CYCLE-LIFE PROFILE A

Assessment Test	Description	SOC	C-Rate
Capacity test:	The amount of energy (in Ah) which may be harnessed from the battery. Determined via coulomb counting	n/a	1C
OCV Test	Discharge the cell from 100% SOC to 0% SOC in 5% decrements at C/2 with an intermittent relaxation period of 4 hours. Record the cell voltage after each rest period.	100% to 0% in 5% decrements	C/2 for SoC adjustments
Electrochemical Impedance Spectroscopy (EIS) Test: 10mHz-10kHz	Internal resistance: Ohmic and direct current resistance (DCR)	10%, 20%, 50%, 80%, 95%	n/a
HPPC Test	Subject cells to HPPC test as described in [13]. Determine ECM model and parameters based on measured current and voltage data.	10%, 20%, 50%, 80%, 95%	20%, 40%, 60%, 80%, 94%
Performance Test	Peak and average cell surface temperature, energy throughput	n/a	HP cycle, IEC cycle

copper cooling fin of 0.5mm thickness. The copper fin itself is contacting a cooling plate through which the coolant medium (water-glycol mixture) is pumped. The temperature set-point of the coolant is set to 20 °C and is controlled by a Lauda unit.

To detect the extent to which cell self-heating occurs for each of the two duty cycles, the cells are equipped with thermocouples to measure cell surface temperatures throughout the experiment. The locations of these thermocouples are shown in Fig. 3.

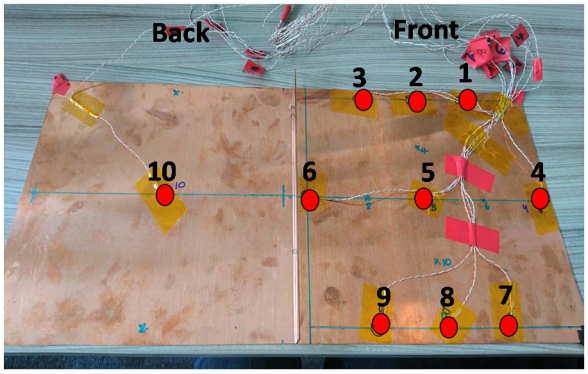

Fig. 3 Position of thermocouples on cooling fin

D. Characterization Tests

Each cell is characterized using the procedures summarized in TABLE I and outline below to determine their discharge capacity at 1C, OCV curve, internal resistance, and temperature during cycling. Furthermore, the data from the Hybrid Pulse Power Characterization test [13] is used to parameterize an equivalent circuit model (ECM) suitable for dynamic modelling of the cell. Between tests, cells are charged using a constant current – constant voltage (CC-CV) protocol. Cells are charged to 4.2V using a current of 26.5 Amperes and charging is complete once the current falls below 2 Ampere.

E. Performance Test

One set of three cells (Cells 1-3) is subjected to HP cycling, the other set (Cells 4-6) is subjected to the IEC-62660 "Cycle-life testing Profile A". Charging currents are limited to 2C to comply with the cell specifications, discharging currents are capped to the test hardware limit of 400 Ampere, which corresponds to 94% of the peak current as specified by the cell manufacturer.

Tests start at 95% SOC and cells are subjected to repetitions of their respective profiles until their state of charge has reached 10% or the safety cut-off temperature of 65°C has been reached. The energy throughput for each cycle is determined from the experimental data, and cell surface temperatures are recorded for all tests.

III. RESULTS AND DISCUSSION

A. Capacity and OCV test

Fig. 4 shows the 1 C discharge Capacity between 100% SoC and 0% SoC for all 6 cells and the mean OCV curve and error bars representing the standard deviation for discharge. There is little variation between cells in terms of discharge capacity and OCV curve. The mean 1C discharge capacity of the cells is 52.01 Ah with a standard error of 0.12. The open circuit voltage of the cells ranges from 4.182 V at 100% SoC to 3.467 V at 0% SoC. The largest deviation of OCV values between cells is 15mV at 0% SOC.

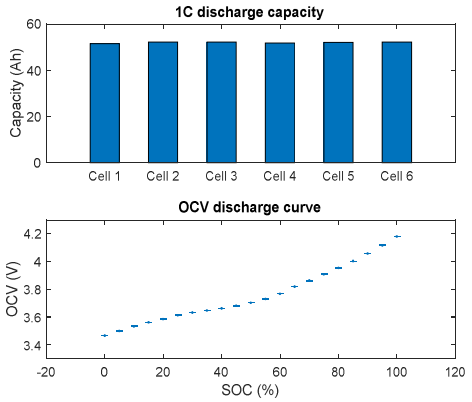

Fig. 4 1C discharge Capacity and OCV curve for discharge

B. EIS Test

The results of the EIS tests for all six cells is shown in the form of Nyquist plots in Fig. 5.

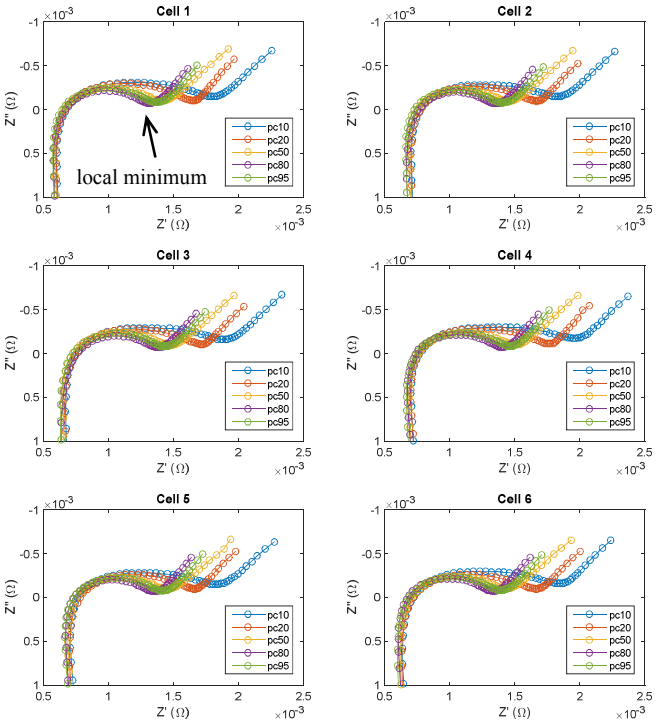

Fig. 5 SOC dependent EIS plots for 6 NCM Cells; pc10 = 10% SoC, etc.

The Nyquist plots recorded for the cells in this work follow the typical shape of those reported in literature, and can be divided into three distinct regions: high-frequency inductive tail, mid-frequency semicircle, and Warburg impedance at low-frequency [14]. The inductive tail in the high frequency region

is associated with conduction through the bulk material of the cell, separator, electrolyte and wires. The pure ohmic resistance can be extracted from the intersection of the inductive trail with the real axis. The semicircle in the mid-frequency region is attributed to charge transfer phenomena and reaction kinetics. The real impedance at the local minimum corresponds with the combined ohmic and charge transfer resistance [15]. Unlike the ohmic resistance, where little SoC dependence may be observed, the charge transfer resistance is largely influenced by the SoC, with higher resistances at high and low states of charge and lower resistance in the middle window. In the low frequency region, the Warburg impedance represents the diffusion limited region in the solid phase of the electrode.

Depending on the use history of the cell, as the batteries degrade with prolonged use, charge-transfer resistance is expected to increase and additional semi-circles associated with cell degradation and SEI growth may be observed [16].

C. HPPC Test

The data extracted from HPPC tests were analyzed in MATLAB using a nonlinear least squares optimization procedure to fit the voltage response of the equivalent circuit model (ECM) displayed in Fig. 6.

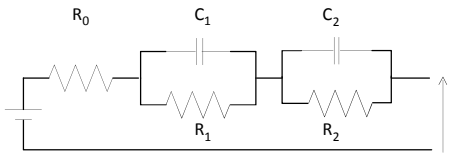

Fig. 6 Equivalent Circuit Model for HPPC data.

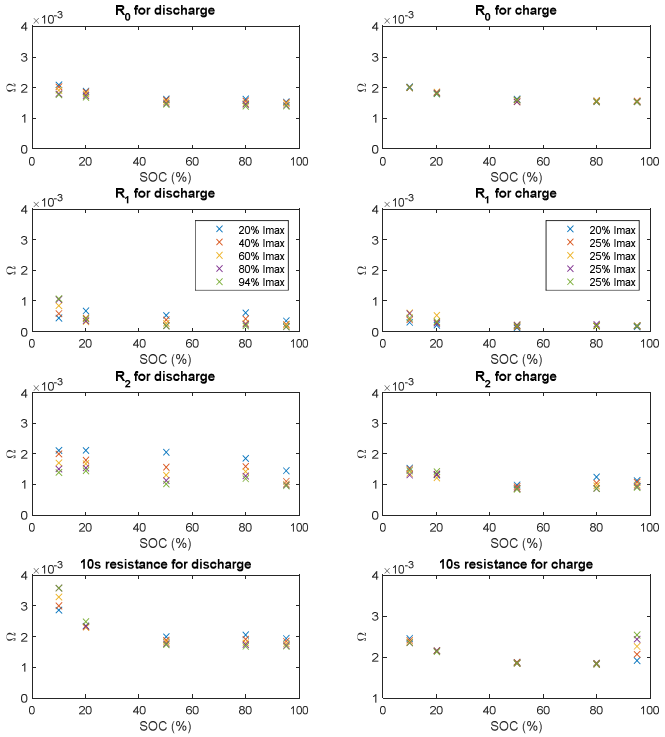

Fig. 7 Current dependent internal resistance of the cells for charging and discharging; Imax corresponds to 424A

The mean values for R_0, R_1, and R_2 as fitted to the ECM as well as the 10s-pulse resistance for charging and discharging as extracted from HPPC tests are displayed in Fig. **7**.

For discharging, the values for R_0 are higher than those found in EIS tests by a factor of 2.5 (EIS ohmic resistance: 0.6-0.7 $m\Omega$, HPPC R_0: 1.4-2.1 $m\Omega$) and show some SoC and current dependency. This observation is attributed to the maximum sampling frequency of the cycler of 10 Hz, corresponding with the mid-frequency measurements from the EIS tests. As such, R_0 is more in line with the combined ohmic and charge transfer resistance from EIS tests. R_1 is more dependent on current and SoC for discharge with high discharge currents at low SoCs returning higher resistance values. The 10s pulse resistance shows both, large current and large SOC dependency. At low SoCs, high discharge currents cause show the highest resistance, whereas at high and medium SoCs only small dependencies may be observed, similarly to the results reported within [17].

Again, charging currents were limited to 2C. As such, little can be said about current dependency of the parameters for charging. However, minor SoC dependencies may be observed for R_1 and R_2, where values at low SoCs are lower than those associated with discharging. The 10s-pulse resistance does show a wide spread at high SoC, which results from the cell reaching its upper voltage limit of 4.2V. The highest resistance value originates from the charging pulse corresponding with the highest discharge current pulse indicating that the cell displays higher charging resistance at high SOCs, as commonly reported [REF].

To simulate the voltage response of a battery using an ECM, the SoC and current dependence of the ECM parameters, as observed in Fig. **7** need to be accounted for.

D. Performance test

Fig. 8 shows the mean temperatures for HP and IEC use cases during a discharge from 95-10% SoC measured by the thermocouples positioned on each cell as shown in Fig. 3.

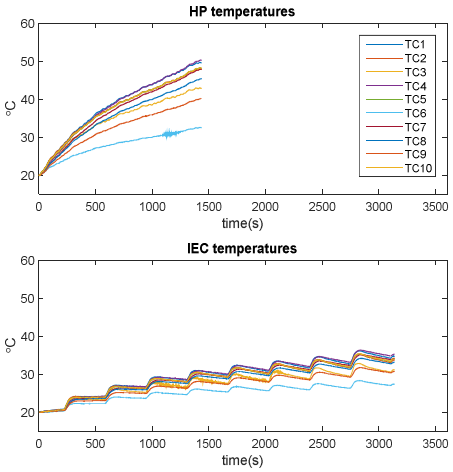

Fig. 8 Thermocouple measurements of cells subjected to the "*HP profile"* (top) and *"IEC Cycle Life Profile A"* (bottom) from 95-10% SoC.

The cells undergoing HP cycling completed 8 repetitions of the HP profile to reach 10% SoC with a mean absolute energy throughput of 68.14 Ah with a standard error of 0.18 Ah, whereas the other cells completed 9 repetitions of the IEC profile with a mean energy throughput of 57.718 Ah and a standard error of 0.003 Ah. As expected, the HP profile results in significantly higher temperatures of up to 51°C and temperature gradients across the cell surface exceeding 19°C for the HP use case compared to a peak temperature of 37°C and temperature gradient of 9°C for the IEC use case.

As high temperatures and temperature gradients are an aggravating factor in cell degradation, it is expected that over prolonged use, cells subjected to the HP profile will experience accelerated degradation compared to cells subjected to the IEC loading profile. Although rate dependent degradation may remain unaffected, adequate thermal management may reduce the extent to which the HP profile degrades the battery cells.

IV. Conclusions and Further work

In this work the characterization of six C-NCM battery cells with a special focus on high performance vehicle use is presented. The peak temperature and temperature gradients across the cell surface during cycling illustrate the evident inability of standardized cycling procedures to account for use cases outside the defined range.

For use cases within the HP vehicle environment existing testing procedures are not sufficient to gather representative data regarding thermal behavior of cells, posing a challenge for battery pack design. Evidently, a cooling system designed using existing standards may not be sufficient for extreme use cases. Equally, a system designed for HP use cases may be over-engineered and inappropriately heavy or expensive. The research presented within this work will be continued in form of long term degradation testing to quantify to what extent the HP use case affects the long-term behavior of a battery cell.

Acknowledgments

The research presented within this paper is supported by the Engineering and Physical Science Research Council through the awards EP/M507593/1 and EP/I01585X/1. The research was undertaken in collaboration with the WMG Centre High Value Manufacturing Catapult (funded by Innovate UK) in collaboration with Jaguar Land Rover and Delta Motorsport.

References

[1] W. Sierzchula, S. Bakker, K. Maat, and B. Van Wee, "The competitive environment of electric vehicles: An analysis of prototype and production models," *Environ. Innov. Soc. Transitions*, vol. 2, pp. 49–65, 2012.

[2] Q. Kellner, W. Dhammika Widanage, and J. Marco, "Battery power requirements in high-performance electric vehicles," in *2016 IEEE Transportation Electrification Conference and Expo (ITEC)*, 2016, pp. 1–6.

[3] L. H. Saw, K. Somasundaram, Y. Ye, and a. a O. Tay, "Electro-thermal analysis of Lithium Iron Phosphate battery for electric vehicles," *J. Power Sources*, vol. 249, pp. 231–238, 2014.

[4] A. Tourani, P. White, and P. Ivey, "Analysis of electric and thermal behaviour of lithium-ion cells in realistic driving cycles," *J. Power Sources*, vol. 268, pp. 301–314, 2014.

[5] S. Chacko and Y. M. Chung, "Thermal modelling of Li-ion polymer battery for electric vehicle drive cycles," *J. Power Sources*, vol. 213, pp. 296–303, 2012.

[6] D. Worwood, Q. Kellner, M. Wojtala, W. D. Widanage, R. McGlen, D. Greenwood, and J. Marco, "A new approach to the internal thermal management of cylindrical battery cells for automotive applications," *J. Power Sources*, vol. 346, pp. 151–166, Apr. 2017.

[7] D. Worwood, E. Hosseinzadeh, Q. Kellner, J. Marco, D. Greenwood, W. McGlen, R., W. Dhammika, A. Barai, and P. A. (Paul A. . Jennings, "Thermal analysis of a lithium-ion pouch cell under aggressive automotive duty cycles with minimal cooling," in *IET Hybrid Electric Vehicle Conference*, 2016, pp. 2–3.

[8] International Electrotechnical Commission, "IEC 62660-1." International Electrotechnical Commission, Geneva, 2010.

[9] J. Schoukens and T. Dobrowiecki, "Design of broadband excitation signals with a user imposed power spectrum and amplitude distribution," in *IEEE Instrumentation and Measurement Technology Conference*, 1998, pp. 1002–1005.

[10] J. Vetter, P. Novák, M. R. Wagner, C. Veit, K.-C. Möller, J. O. Besenhard, M. Winter, M. Wohlfahrt-Mehrens, C. Vogler, and A. Hammouche, "Ageing Mechanisms in lithium-ion batteries," *J. Power Sources*, vol. 147, no. 1–2, pp. 269–281, Sep. 2005.

[11] Y. Troxler, B. Wu, M. Marinescu, V. Yufit, Y. Patel, A. J. Marquis, N. P. Brandon, and G. J. Offer, "The effect of thermal gradients on the performance of lithium-ion batteries," *J. Power Sources*, vol. 247, pp. 1018–1025, 2014.

[12] M. Klett, R. Eriksson, J. Groot, P. Svens, K. Ciosek Högström, R. W. Lindström, H. Berg, T. Gustafson, G. Lindbergh, and K. Edström, "Non-uniform aging of cycled commercial LiFePO4//graphite cylindrical cells revealed by post-mortem analysis," *J. Power Sources*, vol. 257, pp. 126–137, 2014.

[13] Idaho National Laboratory, "U . S . Department of Energy Vehicle Technologies Program Battery Test Manual For Plug-In Hybrid Electric Vehicles," no. December. 2010.

[14] D. Wong, B. Shrestha, D. A. Wetz, and J. M. Heinzel, "Impact of high rate discharge on the aging of lithium nickel cobalt aluminum oxide batteries," *J. Power Sources*, vol. 280, pp. 363–372, Apr. 2015.

[15] W. Waag, S. Käbitz, and D. U. Sauer, "Experimental investigation of the lithium-ion battery impedance characteristic at various conditions and aging states and its influence on the application," *Appl. Energy*, vol. 102, pp. 885–897, 2013.

[16] A. Barai, G. H. Chouchelamane, Y. Guo, A. McGordon, and P. Jennings, "A study on the impact of lithium-ion cell relaxation on electrochemical impedance spectroscopy," *J. Power Sources*, vol. 280, pp. 74–80, Apr. 2015.

[17] Y. Zou, X. Hu, H. Ma, and S. E. Li, "Combined State of Charge and State of Health estimation over lithium-ion battery cell cycle lifespan for electric vehicles," *J. Power Sources*, vol. 273, pp. 793–803, 2015.